Structure-Activity Relationship Study Identifies A Novel Lipophilic Amiloride Derivative That Induces Lysosome-Dependent Cell Death in Therapy-Resistant Breast Cancer Cells

Michelle Hu[1], Ruiwu Liu[1], Kit S. Lam[1], Kermit L. Carraway, III[1]

[1]Department of Biochemistry and Molecular Medicine, and UC Davis Comprehensive Cancer Center, UC Davis School of Medicine, Sacramento, California, USA

***Correspondence:**
Kermit L. Carraway
klcarraway@ucdavis.edu

Keywords: amiloride derivative, lysosomal membrane permeabilization, lysosome-dependent cell death, breast cancer, therapeutic resistance

Abstract

Amiloride and its derivatives have long attracted attention as potential anticancer therapeutic agents. Several early studies characterized amilorides as inhibitors of sodium-proton antiporter-dependent tumor growth and urokinase plasminogen activator-mediated metastasis. However, more recent observations indicate that amiloride derivatives are specifically cytotoxic toward tumor cells relative to normal cells and have the capacity to target tumor cell populations resistant to currently-employed therapies. A major barrier to clinical translation of the amilorides is their modest cytotoxic potency, with EC_{50} values in the high micromolar to low millimolar range. Here we report structure-activity relationship observations that underscore the importance of the guanidinium group and the presence of lipophilic substituents at the C(5) position of the amiloride pharmacophore in promoting cytotoxicity. Moreover, we demonstrate that our most potent derivative called LLC1 is specifically cytotoxic toward mouse mammary tumor organoids and drug-resistant populations of various breast cancer cell lines, and induces lysosomal membrane permeabilization as a prelude to lysosome-dependent cell death. Our observations offer a roadmap for the future development of amiloride-based cationic amphiphilic drugs that engage the lysosome to specifically kill breast tumor cells.

1 Introduction

Amiloride is a commonly employed oral antikaliuretic and diuretic used in the treatment of hypertension and congestive heart failure [1]. Structurally, amiloride is a substituted (pyrazinecarbonyl) guanidine; its relatively high pKa of 8.7 ensures its protonation and function at physiological pH [2-4]. Its renal mechanism of action involves inhibition of both the Na^+/H^+ exchange

34 system of the proximal tubule and the epithelial Na^+ channel of the distal tubule to increase sodium
35 excretion without affecting potassium excretion [3, 4]. In addition to its uses in hypertension and
36 congestive heart failure, amiloride and its numerous derivatives have been studied for a variety of
37 indications, from multiple sclerosis and cystic fibrosis to cancer and chronic pain [5-9].
38
39 While an array of studies since the 1980s have highlighted Na^+/H^+ exchange and urokinase
40 plasminogen activator (uPA) inhibition mechanisms in amiloride suppression of tumor aggressiveness
41 and metastasis [10], more recent observations indicate that amiloride and its derivatives also exhibit
42 tumor cell-selective cytotoxicity via a non-apoptotic mechanism. For example, our studies with the
43 derivative 5-(N,N-hexamethylene)amiloride (HMA) underscore the notion that the properties of
44 amiloride derivatives may be ideally suited for targeting particularly aggressive or therapy-refractory
45 tumors [11, 12]. HMA efficiently kills bulk breast tumor cells independent of subtype, species of
46 origin, or proliferation state, but does not efficiently kill non-transformed cells derived from a variety
47 of tissues at the same concentrations. Indeed, cell lines derived from a variety of tumor types are
48 similarly susceptible to HMA, suggesting that its mechanism of cytotoxic action may be dependent on
49 cellular transformation rather than patient-specific genetic alterations. Moreover, HMA is cytotoxic
50 toward breast cancer cell populations that are resistant to currently-employed therapies, including the
51 highly refractory cancer stem cell population. Finally, HMA induces morphological changes within
52 the lysosomes of tumor cells, and cytotoxicity is rescued by an inhibitor of the lysosomal protease
53 cathepsin [11, 12], pointing a central role for the lysosome in its mechanism of action.
54
55 While previous *in vitro* studies have revealed many attractive properties of amiloride derivatives, and
56 suggest that derivatization of the C(5) position can markedly enhance the tumor-specific cytotoxic
57 properties of the drug, further translation of HMA is hampered by its relatively modest potency and
58 poor pharmacokinetic properties in mice [13]. In this study we aim to glean further insight into

59 structure-activity relationships within the amiloride pharmacophore by comparing the cytotoxic
60 potential of derivatives modified at the C(2) and C(5) positions. Moreover, we aim to identify more
61 potent derivatives that optimize tumor cell-specific cytotoxicity and preserve the ability to target
62 therapy-resistant populations. Finally, we aim to confirm the role of the lysosome in amiloride
63 derivative mechanism of action by characterizing drug impact on lysosomal membrane
64 permeabilization.
65

66 **2 Materials and methods**

67 **2.1 Cell Culture and Drug Treatments**

68 MDA-MB-231, MCF7, SKBR3, T47D, and 4T1 cells were purchased from American Type Culture
69 Collection (ATCC, Manassas, VA, USA) and maintained at 37°C and 10% CO_2 in media supplemented
70 with 10% fetal bovine serum (FBS, Genesee Scientific) and antibiotics (penicillin/streptomycin; Gibco
71 - Thermo Fisher), as recommended by ATCC. MCF7-B7-TS (MCF7 TS), MCF7-G11-TR-1 (MCF7
72 TR-1), MCF7-G11-TR-5 (MCF7 TR-5), and MCF7 MX-100 cells were obtained from the Physical
73 Sciences-Oncology Network (PS-ON) Bioresource Core Facility (PBCF) at ATCC or gifted from Dr.
74 A.M. Yu, UC Davis. The tamoxifen (TAM) resistant lines were maintained in MCF7 base media
75 supplemented with 1 μM or 5 μM TAM [14]. The mitoxantrone resistant line (MX-100) was
76 maintained as described [15]. Cell line attributes are summarized in Supplementary Table S1.
77

78 Amiloride, HMA, benzamil, and 10357 were sourced as described in Supplementary Table S2, and
79 applied to cells to cells at 50-70% confluency. Amiloride derivatives were added 24hr before analysis
80 of cell viability, while chemotherapeutic agents (docetaxel, doxorubicin, and mitoxantrone) were
81 added at specified timepoints to develop short term resistance in parental cell lines. Vehicle was added
82 as a negative control for each experiment.
83

84 **2.2 Design and Synthesis of Novel Amiloride Derivatives**

85 The new amiloride derivatives were designed to introduce novel hydrophobic groups at the C(5)
86 position to improve cell permeability and potential *in vivo* availability. Synthesis of LLC1 was carried
87 out as shown in Supplementary Fig. S1. To a suspension of methyl 3-amino-5,6-dichloro-2-
88 pyrazinecarboxylate (compound 1; 444 mg, 2.0 mmol) in anhydrous DMF (3 mL) was added 4-(4-
89 fluorophenyl)piperidine (compound 2; 358.5 mg, 2.0 mmol) and N,N-*Diisopropylethylamine (*DIPEA,
90 697 μL, 4.0 mmol), the reaction mixture was stirred at room temperature overnight and then added to
91 cold water. The precipitate was collected by centrifuge and washed with water. The crude product
92 (compound 3) was used for the next step without further purification. 0.5 M $NaOCH_3$ solution in
93 CH_3OH (20 mL) was added to guanidine hydrochloride (955.3 mg, 10 mmol) and the resulting mixture
94 was stirred at room temperature for 0.5 hr. The white precipitate was removed by filtration, and the
95 free guanidine solution in methanol was added to a suspension of methyl ester (compound 3; 364.8mg,
96 1.0 mmol) in DMF (5 mL) and stirred at room temperature overnight. Brine (20 mL) was added, and
97 the mixture extracted with ethyl acetate (3 × 30 mL). The organic layer was washed with 10% NaCl (2
98 × 30 mL), dried over anhydrous Na_2SO_4, and concentrated under reduced pressure. The crude mixture
99 was dissolved in 5 mL of 30% CH_3CN/70% H_2O and 0.1% trifluoroacetic acid and purified by a reverse
100 phase HPLC. The collected eluent was lyophilized to yield the designed product LLC1. The structure
101 was verified by Orbitrap HR-ESI MS: 392.1391 [M+1] (Supplementary Fig. S2A). The purity was
102 >98% as shown in HPLC (Supplementary Fig. S2B).

103

104 **2.3 MTT Assay**

105 Cells were seeded on 24-well plates and cultured to 50-70% confluency prior to treatment with various
106 compounds for 24-72hr depending on the assay context. Following treatments, media was aspirated
107 from cells and replaced with 5 mg/mL 3-(4,5-Dimethyl-2-thiazolyl)-2,5-diphenyl-2H-tetrazolium
108 bromide (MTT, #M5655, Sigma Aldrich) solution in base media. Cells were incubated at 37°C for 1-

109 2hr to induce formazan crystal formation, then washed with PBS to remove impurities. Crystals were
110 dissolved using isopropyl alcohol (IPA, 0.5% 1N HCl in isopropanol), and sample absorbance (λ_{ex} 570
111 nm, λ_{em} 655 nm) was measured with a FilterMax F5 microplate reader (Molecular Devices) and Multi-
112 Mode Analysis software (Version 3.4.0.27, Beckman Coulter).
113

114 **2.4 Galectin Translocation Assay**

115 MCF7 cells were plated on glass coverslips in 12-well plates and cultured to 70-80% confluency. Cells
116 were treated with vehicle, 2 mM LLOMe, 40 μM HMA, or 10 μM LLC1 for 12hr and then fixed with
117 4% paraformaldehyde for 10min. After fixation, detection of ruptured lysosomes by galectin-3
118 translocation was evaluated by immunocytochemistry as previously described [16]. Samples were
119 incubated with 50 mM ammonium chloride in PBS for 10min, washed three times with PBS, and then
120 permeabilized and blocked in 1 mL blocking buffer (1% BSA, 0.02% sodium azide, 0.2% NP40, 5%
121 goat serum) at room temperature for 1hr. Cells were incubated with purified mouse anti-human
122 Galectin-3 (1:100 dilution, #556904, BD Biosciences) diluted in blocking buffer for 1hr at room
123 temperature. Cells were washed three times with PBS and then incubated with goat anti-mouse IgG1
124 cross-absorbed secondary antibody Alexa Fluor 488 (1:1,000 dilution, #A-21121, Invitrogen) at room
125 temperature for 1hr. Cells were again washed three times with PBS before incubation with DAPI
126 (1:10,000) in PBS for 10min in the dark and then rinsed twice with PBS twice before mounting with
127 Fluoromount G. Slides were imaged by confocal microscopy using a ZEISS LSM 800 with Airyscan,
128 and galectin-3 puncta formation was analyzed from ten replicate fields with FIJI
129 (https://imagej.net/Fiji) software.
130

131 **2.5 Ex Vivo Drug Cytotoxicity Organoid Assay**

132 Tumor samples were generated from 1 x 10^6 4T1 cells engrafted into Balb/cJ mice (#000651, The
133 Jackson Laboratory) at the 4th mammary fat pad. Tumors (1.0-1.5 cm in diameter) or pooled mammary

134 glands from Balb/cJ mice were harvested and chopped into fine pieces using a razor blade before
135 addition to digestion buffer (DMEM/F12 #SH30023, HyClone;1% PenStrep, Gibco - Thermo Fisher;
136 2% FBS, Genesee Scientific; collagenase/hyaluronidase (5%: tumors & 10%: mammary glands),
137 #07912, StemCell Technologies; 5ug/mL insulin, Gibco - Thermo Fisher) and vortexed. Samples were
138 digested for 2hr at 37°C under gentle shaking, and samples vortexed every 30min, before they were
139 processed. After neutralization of the digestion buffer with DMEM (Gibco - Thermo Fisher) containing
140 10% FBS, organoids were centrifuged at 700rpm to remove cellular debris. ACK lysis buffer (Gibco -
141 Thermo Fisher) was used to remove red blood cells from the organoids. A quick spin was performed
142 to remove additional debris and to pellet organoids. Once resuspended in PBS, organoids were
143 embedded into MatriGel (#354230, Corning) and cultured in organoid growth media (OGM) on 24-
144 well plates for 24hr as described previously [17]. After overnight incubation in OGM, organoids were
145 treated with vehicle or 10 μM LLC1 for up to 72hr, and viability was measured using RealTime Glo
146 (#G9711, Promega) according to manufacturer's instructions. Images were taken before drug treatment
147 (0hr) and every 24hr over the course of drug treatment. Representative brightfield images were taken
148 with an Olympus IX81 microscope with CellSens Entry software. Chemiluminescent images were
149 taken with a ChemiDoc Touch Imaging System (BioRad) and analyzed with FIJI
150 (https://imagej.net/Fiji) software to quantify RealTime Glo signal.
151

152 **2.6 Statistical, Data, and Image Analysis**

153 A minimum of three replicates per experiment was performed with values calculated and expressed as
154 averages, unless otherwise stated. P-values of less than 0.05 were considered statistically significant
155 using a student's t-test. Data analysis was performed using Microsoft Excel or GraphPad Prism version
156 9.3.1 for Windows (GraphPad Software; San Diego, CA, USA; www.graphpad.com). Images were
157 compiled in Microsoft PowerPoint and only brightness and contrast were altered for clarity.
158

159 **3 Results**

160 **3.1 Addition of lipophilic substituents to amiloride C(2) and C(5) positions increases cytotoxic**
161 **potency**

162 Amiloride is often modified at the C(2), C(5), and C(6) positions of the pyrazine ring (see Fig. 1A) to
163 improve its transporter inhibition activity and selectivity [7, 18], and such derivatives have been
164 employed to assess the contribution of ion channel function to tumor growth and progression [8, 10,
165 11, 13, 19-28]. However, our recent studies indicating that the amiloride derivative HMA can provoke
166 the non-apoptotic death of tumor cells relative to non-cancer cells by acting via the lysosome [11, 12]
167 prompt the question of whether these cytotoxic properties might be further optimized.

168

169 As HMA adds a lipophilic hexamethylene group to the core pharmacophore at the C(5) position, we
170 first asked whether lipophilic modification increases the cytotoxic potency of amiloride using
171 immediately available amiloride derivatives. Fig. 1 depicts the structures of parent drug amiloride (Fig.
172 1A), C(2) derivative benzamil (Fig. 1B), C(5) derivative HMA (Fig. 1C), and C(5) derivative 10357
173 (Fig. 1D) [26], and summarizes the cytotoxic potency of these derivatives toward cell lines representing
174 ER/PR-positive (MCF7), HER2-positive (SKBR3) and triple-negative (MDA-MB-231) breast tumor
175 subtypes in an MTT cell viability assay (Fig. 1E). Consistent with previous observations [11, 22, 23,
176 27, 29, 30], we observed that amiloride modification with various lipophilic substituents at the C(2) or
177 C(5) position markedly augments cytotoxicity, strongly suggesting that access to an intracellular
178 target(s) is key to drug mechanism of action.

179

180 **3.2 Novel amiloride derivatives underscore the importance of the guanidinium group**

181 To more rigorously test the link between amiloride derivative lipophilicity and cytotoxic potential, we
182 synthesized nine amiloride derivatives, all modified with various substituents at the C(5) position. The
183 structures and EC_{50} values for cytotoxicity toward the three breast cancer cell line models are

184 summarized in Table 1, and the chemical characteristics of all derivatives ordered by EC_{50} are
185 summarized in Table 2. Three key points emerge from comparisons of these derivatives. First, Table 2
186 suggests a strong correlation between cytotoxic efficacy and lipophilicity, reflected in partition
187 coefficient (logP) values of the derivatives. For example, LLC1 and 10357, which exhibit some of the
188 highest logP values (2.46 and 2.88, respectively) among the group, also exhibit the most potent
189 cytotoxicity toward the breast cancer cell lines (5-13 μM and 9-17 μM, respectively). On the other
190 hand, the low logP values for amiloride and LLC10 (-0.89 and -0.28, respectively) correlate with
191 particularly poor cytotoxicity (148-995 μM and 883-2732 μM, respectively). Second, a direct
192 comparison of derivatives LLC1 and LLC3 (Table 1) illustrates the importance of maintaining the
193 integrity of the C(2) guanidinium structure. Both derivatives contain an identical lipophilic C(5)
194 substituent, but the removal of one of the guanidinium amines correlates with a 6-16 fold decrease in
195 cytotoxic potency. Finally, to a first approximation derivatives tend to act with similar potency toward
196 all three cell lines (Table 1). This suggests that, consistent with previous observations [11, 12],
197 amiloride derivatives act with similar efficacy toward the different breast cancer subtypes. These
198 observations reveal new parameters for the optimization of amiloride derivatives, and highlight LLC1
199 as a novel lead.
200

201 **3.3 LLC1 reduces the viability of murine mammary tumor organoids ex vivo**

202 We have previously demonstrated that HMA reduces the viability of organoids derived from the PymT
203 and NDL genetically-engineered mouse models of breast cancer [12]. To determine whether LLC1 is
204 selectively cytotoxic toward mammary tumors *ex vivo*, we compared its impact on tumor and normal
205 mammary gland organoids generated from Balb/cJ mice orthotopically engrafted with 4T1 (ER^-/PR^-
206 $/HER2^-$), a murine mammary cancer cell line. The approximate EC_{50} value of LLC1 toward human
207 tumor cell lines (10 μM, Table 1) was used to compare the efficiency of cell death as a function of
208 time. We observed that while tumor organoids markedly shrink over 72 hours of treatment (Figs. 2A

209 and 2B), normal mammary gland organoids are resistant to LLC1 treatment (Figs. 2C and 2D). These
210 observations suggest that, similar to its predecessor HMA [11, 12], LLC1 exhibits significant
211 selectivity toward cancer cells and leaves untransformed cells largely unharmed.
212
213 **3.4 HMA and LLC1 act on therapy-resistant breast cancer cell populations**
214 Our previous observations indicate that HMA is cytotoxic toward 'persister' populations of breast
215 cancer cells that survive 3-9 day exposure to conventional chemotherapeutic agents cisplatin, docetaxel
216 and doxorubicin [12]. To confirm HMA's capabilities and test LLC1's properties, we examined the
217 impact of both drugs on the viability of various breast cancer cell line models of short-term and
218 established therapeutic resistance. We first examined the response of therapy-resistant populations of
219 MDA-MB-231 cells toward the derivatives. In the experiment shown in Fig. 3, cells were first
220 pretreated for 48 hours with DMSO vehicle, and then further treated for 24 hours with DMSO, 250 nM
221 DTX, 5 μM DOXO, and either 40 μM HMA (Fig. 3A) or 10 μM LLC1 (Fig. 3D). In each case, drug
222 treatment tended to lower cell viability, confirming that the drugs behave as expected. However, in
223 cells pretreated for 48 hours with either DTX (Figs. 3B and 3E) or DOXO (Figs. 3C and 3F), a second
224 challenge with the pretreating drug did not reduce viability while HMA or LLC1 treatment was
225 cytotoxic.
226
227 We further observed that roughly half of T47D cells, an ER/PR$^+$ breast cancer cell line, exhibit
228 resistance to cell death induced by 72 hour treatment with doxorubicin (DOXO, Fig. 4A) and docetaxel
229 (DTX, Fig. 4D), reflected in the inability of high doses of either drug to further impact viability in a
230 titration. However, we found that both HMA and LLC1 are cytotoxic toward the residual this
231 population that remains after chemotherapeutic treatment, and exhibit similar EC_{50} values as cell lines
232 representing a variety of solid tumor types (Figs. 3B, 3C and 3E, 3F; refs [11, 12]).
233

234 Finally, to assess amiloride derivative effect on a model of sustained drug resistance, we examined the
235 impact of HMA and LLC1 on MCF7 cells selected for long-term resistance to tamoxifen (TAM), an
236 estrogen modulator, and mitoxantrone (MX), a DNA damaging agent [31-34]. Parental MCF7 and
237 MCF7 MX-100, a derivative selected for stable MX resistance that overexpresses ABCG2 (aka breast
238 cancer resistance pump, BCRP) by 30-fold, and MCF TS (tamoxifen sensitive derivative) and MCF7
239 TR-1 and MCF7 TR-5 (tamoxifen resistant derivatives), were treated with varying concentrations of
240 TAM, DTX, DOXO, HMA, and LLC1 and cytotoxicity EC_{50} values were determined (Table 3). We
241 observed that parental MCF7 cells are 3-13 fold more sensitive to chemotherapeutic agents DTX and
242 DOXO than MX-100, but both cell lines are similarly sensitive to HMA and LLC1. Likewise, MCF7
243 TS cells are far more sensitive to tamoxifen than MCF7 TR-1 and MCF7 TR-5 cells, but all three lines
244 ae similarly sensitive to HMA and LLC1. Collectively, these observations provide strong evidence that
245 amiloride derivatives act on breast tumor cell populations that are resistant to clinically pertinent anti-
246 cancer agents.
247

248 **3.5 HMA and LLC1 cause lysosomal membrane permeabilization in resistant breast cancer**
249 **lines**

250 We have previously demonstrated that HMA induces disrupts lysosomal morphology and that drug-
251 induced cell death is rescued by inhibition of the lysosomal protease cathepsin [11]. These observations
252 raise the possibility that amiloride derivatives act by inducing lysosomal membrane permeabilization
253 (LMP), and that the resulting release of cathepsin into the cytosol triggers the non-apoptotic lysosomal
254 cell death pathway. To determine whether the amilorides might act via this mechanism we employed
255 a sensitive galectin translocation assay [16], which measures the accumulation of diffusely distributed
256 cytosolic and nuclear galectin protein to punctate lysosomes upon LMP [35], to assess drug-induced
257 lysosomal disruption. In the experiments depicted in Fig. 5, MCF7 TR-5 cells were treated with for 12
258 hours with 2mM LLOMe (a potent LMP inducer used here as a positive control, refs [[35, 36]), 40 μM

259 HMA, or 10 μM LLC1, and galectin localization was imaged by confocal fluorescence microscopy.
260 We observed that both HMA and LLC1 induce the relocalization of galectin to lysosomes in MCF7
261 TR-5 cells (Fig. 5A), quantitatively reflected in an increase in the total number of puncta per cell (Fig.
262 5B), a loss in the percentage of cells exhibiting 0 puncta, and gains in the percentages of cells exhibiting
263 either 1-5 puncta or 6 or more puncta (Fig. 5C). A quantitative comparison of galectin relocalization
264 in MCF7 TS and MCF7 TR-1 (see Supplementary Figs. S3 & S4) to MCF7 TR-5 cells revealed that
265 both HMA and LLC1 similarly induce LMP in all three lines (Figs. 5D-5G). These observations
266 indicate that amiloride derivatives compromise the integrity of lysosomes, which in turn could
267 significantly contribute to their cytotoxic mechanism. Moreover, this process appears to be similarly
268 engaged in sensitive and drug-resistant cells, possibly accounting for the activity of these agents toward
269 resistant populations.
270

271 **4 Discussion**

272 Amiloride derivatives exhibit significant promise as cancer therapeutics because they have the potential
273 to eradicate therapy-resistant populations of breast cancer through permeabilization of the lysosome
274 and engagement of lysosome-dependent cell death (LDCD). The optimization of amiloride structure is
275 an enticing area for medicinal chemists and biologists alike because the relative ease of synthesis and
276 chemical modification allows the straightforward development of new derivatives, while optimizing
277 its unique anticancer properties. This study reveals that LLC1, a novel lipophilic C(5) amiloride
278 derivative, induces cell death in the single digit micromolar range, selectively kills tumor organoids
279 relative to normal mammary gland organoids, and acts to induce LMP. These observations suggest that
280 LLC1 has potential clinical applicability and warrants further testing and optimization as a lead
281 compound.
282

283 Our structure-activity relationship analysis provides key insight into building more effective cancer-
284 selective cytotoxic amiloride derivatives. First, we observe a strong relationship between amiloride
285 lipophilicity, reflected in more positive logP values, and drug cytotoxicity. Indeed, our most potent
286 derivative LLC1 exhibits one of the highest logP values of the compounds we have examined,
287 suggesting that improving lipophilicity further could result in even more effective drug leads. These
288 conclusions dovetail with current trends in drug development that prioritize more lipophilic drugs
289 because of their higher likelihood of passing safety and ADME concerns during Phase 1 clinical studies
290 [37]. At the same time, disruption of the guanidinium moiety at the C(2) position appears deleterious
291 to cytotoxic function. LLC1 and LLC3 are identical except for the deletion of one of the guanidinium
292 amino groups in LLC3, and this change leads to an order of magnitude loss of potency. In this regard
293 it might be interesting to determine whether lipophilic derivatives of other existing guanidinium-
294 containing drugs such as metformin might also exhibit tumor cell-selective cytotoxicity.
295
296 More broadly, this concept can be further applied to cationic amphiphilic drugs (CADs) which are
297 defined by their ability to accumulate in lysosomes because of their lipophilic nature and amine-
298 containing structures [38, 39]. As amiloride derivatives fall under the CAD family, it would be of
299 interest to perform screens such as that described by Pagliero et al. to assess the efficiency of LMP
300 initiation by newly synthesized C(5) amiloride derivatives relative to cytotoxicity EC_{50} values [40].
301 The use of omics and biochemical approaches could also prove fruitful in finding putative direct targets
302 of amiloride derivative action.
303
304 **Data availability statement**
305 The original contributions presented in the study are included in the article/Supplementary Material,
306 further inquiries may be directed to the corresponding author.
307

308 **Author contributions**

309 Conceptualization: KLC; methodology: MH, RL; validation: MH; formal analysis: MH;
310 investigation: MH; resources: RL, KSL; writing-original draft preparation: MH; writing-review and
311 editing: MH, RL, KLC; visualization: MH; supervision: KSL, KLC; funding acquisition: KLC. All
312 authors have read and agreed to the published version of the manuscript.

313

314 **Conflict of interest**

315 The authors declare that the research was conducted in the absence of any commercial or financial
316 relationships that could be construed as a potential conflict of interest.

317

318 **Supplementary material**

319 The Supplementary Material for this article may be found online at:

320

321 **Acknowledgments**

322 We thank Dr. Frederic Gorin for providing compound 10357 and Dr. Aiming Yu for providing the
323 MX-100 MCF7 derivative cell line. These studies were supported by NIH/NCI grants R01CA250211
324 and R01CA230742 (KLC). The Combinatorial Chemistry and Chemical Biology shared resource is
325 supported by NIH/NCI Cancer Center Support Grant P30CA093373.

326

327 **References**

328 1. Mazzo, D.J., *Amiloride Hydrochloride*, in *Analytical Profiles of Drug Substances*, K. Florey,
329 Editor. 1986. p. 1-34.
330 2. Palmer, L.G. and T.R. Kleyman, *Potassium-Retaining Diuretics: Amiloride*, in *Diuretics*, R.F.
331 Greger, H. Knauf, and E. Mutschler, Editors. 1995, Springer Berlin Heidelberg: Berlin,
332 Heidelberg. p. 363-394.
333 3. Baer, J.E., et al., *The Potassium-Sparing and Natriuretic Activity of N-Amidino-3,5-Diamino-*
334 *6-Chloropyrazinecar-Boxamide Hydrochloride Dihydrate (amiloride Hydrochloride).* Journal
335 of Pharmacology and Experimental Therapeutics, 1967. **157**(2): p. 472-485.
336 4. Frelin, C., et al., *Molecular properties of amiloride action and of its Na+ transporting*
337 *targets.* Kidney Int, 1987. **32**(6): p. 785-93.

338 5. Arun, T., et al., *Targeting ASIC1 in primary progressive multiple sclerosis: evidence of*
339 *neuroprotection with amiloride.* Brain, 2013. **136**(Pt 1): p. 106-15.
340 6. Hirsh, A.J., et al., *Evaluation of second generation amiloride analogs as therapy for cystic*
341 *fibrosis lung disease.* J Pharmacol Exp Ther, 2004. **311**(3): p. 929-38.
342 7. Kleyman, T.R. and E.J. Cragoe, Jr., *Amiloride and its analogs as tools in the study of ion*
343 *transport.* J Membr Biol, 1988. **105**(1): p. 1-21.
344 8. Harguindey, S., et al., *Proton Transport Inhibitors as Potentially Selective Anticancer Drugs.*
345 Anticancer Research, 2009. **29**(6): p. 2127-2136.
346 9. Kuduk, S.D., et al., *Amiloride derived inhibitors of acid-sensing ion channel-3 (ASIC3).*
347 Bioorg Med Chem Lett, 2009. **19**(9): p. 2514-8.
348 10. Matthews, H., M. Ranson, and M.J. Kelso, *Anti-tumour/metastasis effects of the potassium-*
349 *sparing diuretic amiloride: an orally active anti-cancer drug waiting for its call-of-duty?* Int J
350 Cancer, 2011. **129**(9): p. 2051-61.
351 11. Rowson-Hodel, A.R., et al., *Hexamethylene amiloride engages a novel reactive oxygen*
352 *species- and lysosome-dependent programmed necrotic mechanism to selectively target*
353 *breast cancer cells.* Cancer Lett, 2016. **375**(1): p. 62-72.
354 12. Berg, A.L., et al., *The Cationic Amphiphilic Drug Hexamethylene Amiloride Eradicates Bulk*
355 *Breast Cancer Cells and Therapy-Resistant Subpopulations with Similar Efficiencies.*
356 Cancers, 2022. **14**(4): p. 949.
357 13. Luo, J. and I.F. Tannock, *Inhibition of the regulation of intracellular pH: potential of 5-(N,N-*
358 *hexamethylene) amiloride in tumour-selective therapy.* Br J Cancer, 1994. **70**(4): p. 617-24.
359 14. Lyu, Y., et al., *Development of a Cationic Amphiphilic Helical Peptidomimetic (B18L) As A*
360 *Novel Anti-Cancer Drug Lead.* Cancers, 2020. **12**(9): p. 2448.
361 15. Li, X., et al., *Bioengineered miR-27b-3p and miR-328-3p modulate drug metabolism and*
362 *disposition via the regulation of target ADME gene expression.* Acta Pharmaceutica Sinica.
363 B, 2019. **9**(3): p. 639-647.
364 16. Aits, S., M. Jaattela, and J. Nylandsted, *Methods for the quantification of lysosomal*
365 *membrane permeabilization: a hallmark of lysosomal cell death.* Methods Cell Biol, 2015.
366 **126**: p. 261-85.
367 17. Nguyen-Ngoc, K.V., et al., *ECM microenvironment regulates collective migration and local*
368 *dissemination in normal and malignant mammary epithelium.* Proceedings of the National
369 Academy of Sciences, 2012. **109**(39): p. E2595-E2604.
370 18. Li, J.H., E.J. Cragoe, Jr., and B. Lindemann, *Structure-activity relationship of amiloride*
371 *analogs as blockers of epithelial Na channels: I. Pyrazine-ring modifications.* J Membr Biol,
372 1985. **83**(1-2): p. 45-56.
373 19. Garcia-Canero, R., et al., *Na+ :H+ exchange inhibition induces intracellular acidosis and*
374 *differentially impairs cell growth and viability of human and rat hepatocarcinoma cells.*
375 Toxicol Lett, 1999. **106**(2-3): p. 215-28.
376 20. Aredia, F., et al., *Multiple effects of the Na(+)/H (+) antiporter inhibitor HMA on cancer*
377 *cells.* Apoptosis, 2013. **18**(12): p. 1586-98.
378 21. Harguindey, S., et al., *Cariporide and other new and powerful NHE1 inhibitors as potentially*
379 *selective anticancer drugs--an integral molecular/biochemical/metabolic/clinical approach*
380 *after one hundred years of cancer research.* J Transl Med, 2013. **11**: p. 282.
381 22. Leon, L.J., et al., *A cell-permeant amiloride derivative induces caspase-independent, AIF-*
382 *mediated programmed necrotic death of breast cancer cells.* PLoS One, 2013. **8**(4): p.
383 e63038.
384 23. Pasupuleti, N., et al., *5-Benzylglycinyl-amiloride kills proliferating and nonproliferating*
385 *malignant glioma cells through caspase-independent necroptosis mediated by apoptosis-*
386 *inducing factor.* J Pharmacol Exp Ther, 2013. **344**(3): p. 600-15.

24. Amith, S.R., J.M. Wilkinson, and L. Fliegel, *KR-33028, a potent inhibitor of the Na(+)/H(+) exchanger NHE1, suppresses metastatic potential of triple-negative breast cancer cells.* Biochem Pharmacol, 2016. **118**: p. 31-39.
25. Gorin, F.A., et al., *Killing Glioma 'Stem-like' Cells via Drug-Induced Relocation of Endosomal Urokinase Proteins.* Anticancer Agents Med Chem, 2017. **17**(1): p. 40-47.
26. Gorin, F., *Intracellular Urokinase uPA-PAl-1 Complex: Disruption by Small Molecule Targets Hypoxically Programmed Glioma Cells.* Open Access Journal of Neurology & Neurosurgery, 2018. **7**(3): p. 18.
27. Buckley, B.J., et al., *6-Substituted Hexamethylene Amiloride (HMA) Derivatives as Potent and Selective Inhibitors of the Human Urokinase Plasminogen Activator for Use in Cancer.* J Med Chem, 2018. **61**(18): p. 8299-8320.
28. Buckley, B.J., et al., *Systematic evaluation of structure–property relationships and pharmacokinetics in 6-(hetero)aryl-substituted matched pair analogs of amiloride and 5-(N,N-hexamethylene)amiloride.* Bioorganic & Medicinal Chemistry, 2021. **37**: p. 116116.
29. Lee, Y.S., M.M. Sayeed, and R.D. Wurster, *Intracellular Ca2+ mediates the cytotoxicity induced by bepridil and benzamil in human brain tumor cells.* Cancer Lett, 1995. **88**(1): p. 87-91.
30. Shono, Y., et al., *Change in Intracellular pH Causes the Toxic Ca2+ Entry via NCX1 in Neuron- and Glia-Derived Cells.* Cellular and Molecular Neurobiology, 2010. **30**(3): p. 453-460.
31. Lumachi, F., D.A. Santeufemia, and S.M. Basso, *Current medical treatment of estrogen receptor-positive breast cancer.* World J Biol Chem, 2015. **6**(3): p. 231-9.
32. Sazgarnia, A., et al., *In vitro survival of MCF-7 breast cancer cells following combined treatment with ionizing radiation and mitoxantrone-mediated photodynamic therapy.* Photodiagnosis and Photodynamic Therapy, 2013. **10**(1): p. 72-78.
33. Dorssers, L.C.J., et al., *Tamoxifen Resistance in Breast Cancer.* Drugs, 2001. **61**(12): p. 1721-1733.
34. Gupta, A., et al., *Cyclosporin A, tacrolimus and sirolimus are potent inhibitors of the human breast cancer resistance protein (ABCG2) and reverse resistance to mitoxantrone and topotecan.* Cancer Chemotherapy and Pharmacology, 2006. **58**(3): p. 374-383.
35. Aits, S., et al., *Sensitive detection of lysosomal membrane permeabilization by lysosomal galectin puncta assay.* Autophagy, 2015. **11**(8): p. 1408-1424.
36. Uchimoto, T., et al., *Mechanism of apoptosis induced by a lysosomotropic agent, L-Leucyl-L-Leucine methyl ester.* APOPTOSIS, 1999. **4**(5): p. 357-362.
37. Lobo, S., *Is there enough focus on lipophilicity in drug discovery?* Expert Opinion on Drug Discovery, 2020. **15**(3): p. 261-263.
38. Kazmi, F., et al., *Lysosomal sequestration (trapping) of lipophilic amine (cationic amphiphilic) drugs in immortalized human hepatocytes (Fa2N-4 cells).* Drug Metab Dispos, 2013. **41**(4): p. 897-905.
39. Hu, M. and K.L. Carraway, III, *Repurposing Cationic Amphiphilic Drugs and Derivatives to Engage Lysosomal Cell Death in Cancer Treatment.* Frontiers in Oncology, 2020. **10**.
40. Pagliero, R.J., et al., *Discovery of Small Molecules That Induce Lysosomal Cell Death in Cancer Cell Lines Using an Image-Based Screening Platform.* Assay Drug Dev Technol, 2016. **14**(8): p. 489-510.

TABLES

Name	MDA-MD-231 EC_{50}	MCF7 EC_{50}	SKBR3 EC_{50}	Structure
LLC1	7 μM ± 0.4	13 μM ± 2	5 μM ± 0.6	R_1= R_2= 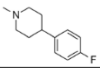
LLC2	43 μM ± 5	54 μM ± 5	97 μM ± 10	R_1= R_2=
LLC3	114 μM ± 25	75 μM ± 28	46 μM ± 6	R_1= R_2= 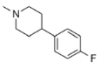
LLC4	40 μM ± 5	56 μM ± 17	34 μM ± 4	R_1= R_2= 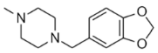
LLC5	18 μM ± 1	29 μM ± 4	10 μM ± 0.6	R_1= R_2=
LLC7	111 μM ± 41	138 μM ± 58	129 μM ± 23	R_1= R_2=
LLC8	90 μM ± 11	75 μM ± 9	74 μM ± 7	R_1= R_2=
LLC9	52 μM ± 7	55 μM ± 11	53 μM ± 7	R_1= R_2= 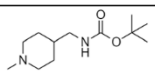
LLC10	3 mM ± 1	1 mM ± 3	0.9 mM ± 0.4	R_1= R_2= 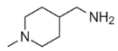

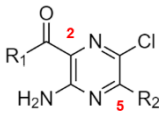

Table 1. Potencies of novel 2- & 5-substituted amiloride derivatives. The core pharmacophore with positions of the two R groups is depicted to the right, while EC_{50} data (from MDA-MB-231, MCF7, and SKBR3 cells) and specific R groups for each compound are represented in the table. Data are compiled from three biological replicates of each cell line.

Name	Rule of 5	PSA (Å²)	Pol (Å³)	MR (cm³/mol)	Acidic pKa	Basic pKa	PI	LogP	HLB	Sol (mg/ml)	Sol Level	IC_{50} (μM)
LLC1	Y	136.51	37.29	103.42	14.85	7.12	10.98	2.46	11.477	0.015	Moderate	5-13
10357	Y	142.5	39.64	102.68	14.85	5.46	10.15	2.877	11.712	0.001	Low	9-17
LLC5	Y	136.51	33.88	94.34	14.85	7.1	10.97	1.811	12.4	0.037	Moderate	10-29
HMA	Y	136.51	29.94	83.16	14.85	7.1	10.97	1.342	13.109	0.188	High	18-36
LLC4	N	158.21	41.7	112.85	14.85	7.15	10.99	1.241	20.051	0.06	Moderate	34-56
LLC9	Y	174.84	41.1	111.49	14.5	7.12	10.76	1.21	17.68	0.121	High	52-55
LLC2	Y	136.51	31.01	86.18	14.85	7.12	10.98	0.905	12.697	0.152	High	43-97
Benzamil	Y	145.3	31.01	86.08	14.68	7.42	11.04	1.112	13.059	0.073	High	50-114
LLC3	Y	110.16	34.8	97.56	12.47	2.68	7.57	2.834	16.875	0.018	Moderate	46-114
LLC8	Y	136.51	27.86	79.52	14.85	7.13	10.99	0.691	13.7	0.263	High	74-90
LLC7	Y	171.31	31.46	86.21	14.47	9.89	12.13	0.029	18.857	0.215	High	111-138
Amiloride	Y	159.29	19.74	56.69	14.85	7.29	11.06	-0.89	15.933	2.768	High	148-995
LLC10	Y	162.53	31.46	86.62	14.85	10.22	12.53	-0.282	19.225	1.1	High	883-2732

Table 2. Chemical and cytotoxicity characteristics of amiloride derivatives. The chemical properties of the novel amiloride derivatives are ordered according to increasing collective cytotoxicity EC_{50} toward MCF7, SKBR3 and MDA-MB-231 breast cancer cell lines. All of the chemical data [Rule of 5, topological polar surface area (PSA), polarizability (Pol), molar refractivity (MR), acidic pKa, basic pKa, isoelectric point (PI), logP, hydrophilic-lipophilic balance (HLB), intrinsic solubility (Sol), and solubility level (Sol level)], were obtained with Chemicalize [July 2022]; https://chemicalize.com/, developed by ChemAxon.

	DTX (μM)	DOXO (μM)	HMA (μM)	LLC1 (μM)
MCF7	1 ± 0.6	2 ± 0.3	27 ± 2	13 ± 2
MCF7 MX-100	13 ± 3	7 ± 0.5	39 ± 3	12 ± 1

	TAM (μM)	HMA (μM)	LLC1 (μM)
MCF7 TS	13 ± 1	68 ± 3	25 ± 0.9
MCF7 TR-1	>10*	67 ± 4	26 ± 2
MCF7 TR-5	>10*	59 ± 5	19 ± 2

451

452

453 **Table 3. MCF7 chemoresistant cells are susceptible to HMA and LLC1 but not conventional**
454 **chemotherapeutics.** A table illustrating the variety of MCF7-chemoresistant cells treated with their
455 respective chemotherapeutic (tamoxifen (TAM) or mitoxantrone (MX)), HMA, or LLC1 for 24hr to
456 determine their EC50 values. An asterisk denoted by a value indicated the EC_{50} value could not be
457 calculated and is the high dose used to treat the cells. Data is represented from a minimum of three
458 independent studies.

459

460

461 **FIGURES**

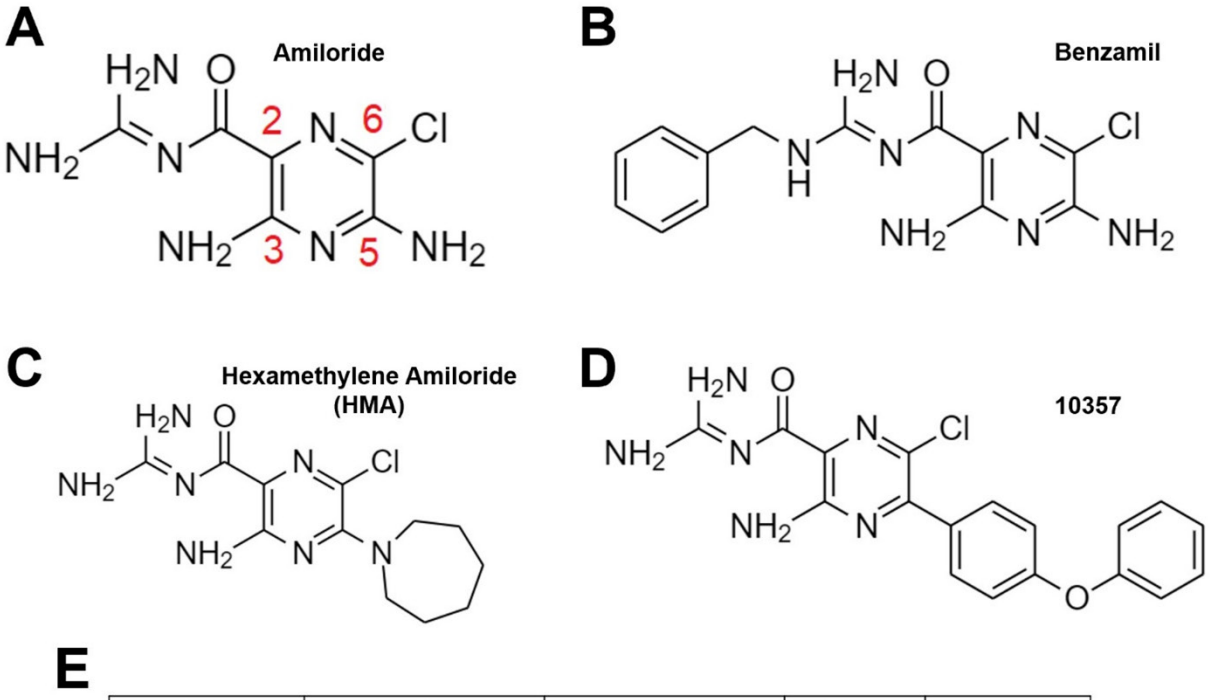

E

EC_{50}	Amiloride (μM)	Benzamil (μM)	HMA (μM)	10357 (μM)
MDA-MB-231	398 ± 44	114 ± 32	36 ± 2	17 ± 2
MCF7	995 ± 341	56 ± 12	27 ± 2	15 ± 2
SKBR3	148 ± 15	50 ± 6	18 ± 1	9 ± 0.7

462

463 **Figure 1. Modification of amiloride with lipophilic substituents enhances its cytotoxic potency.**

464 **(A)** Structure of amiloride with its key carbons numbered. **(B-D)** 2- and 5-substituted amiloride

465 derivatives. **(E)** Cytotoxic potency of amilorides toward cultured breast cancer cell lines.

466

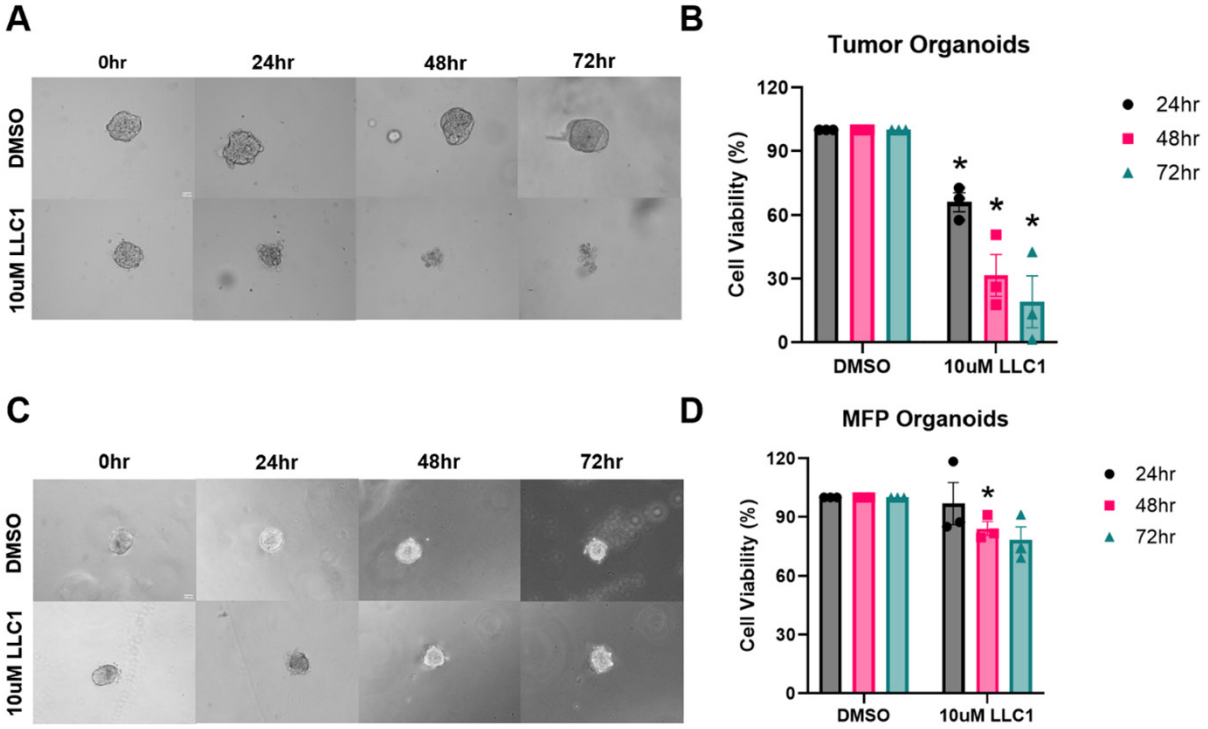

Figure 2. LLC1 selectively reduces viability of mouse mammary tumors *ex vivo*. Representative images of organoids generated from mammary tumors **(A)** and normal mammary glands **(C)** of 4T1-engrafted Balb/cJ mice are shown. Scale bar = 100 µm. **(B, D)** Organoids were treated with 10 µM LLC1, and viability was assessed using RealTime Glo over 72hr and normalized to vehicle (DMSO). Tumor **(B)** or mammary fat pad (MFP) **(D)** organoid viability was monitored every 24hr. Data was compiled from three biological replicates of organoids derived from tumors or mammary glands of independent mice.

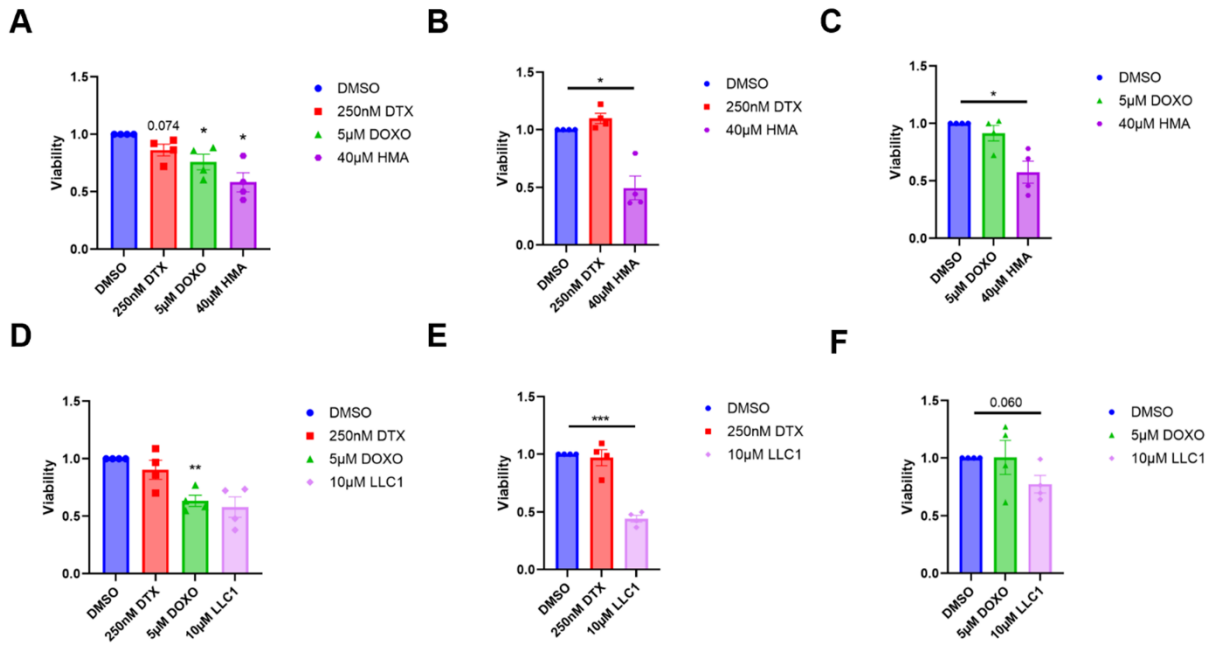

476

477 **Figure 3. LLC1 is cytotoxic toward chemoresistant triple-negative breast cancer cell populations.**

478 **(A,D)** MDA-MD-231 cells were initially treated with DMSO for 48hr, followed by a second challenge

479 with DMSO, 250 nM docetaxel (DTX), 5 μM doxorubicin (DOXO), and either 40 μM HMA **(A)** or

480 10 μM LLC1 **(D)** for 24hr, and then cell viability was determined. **(B,E)** Following 48hr 250 nM DTX

481 **(B, E)** or 5 μM DOXO **(C, F)** pretreatment, the residual population was treated with vehicle, initial

482 chemotherapy treatment (DOXO or DTX), HMA **(B, C)**, or LLC1 **(E, F)** for an additional 24hr. Data

483 is represented from a minimum of four independent studies.

484

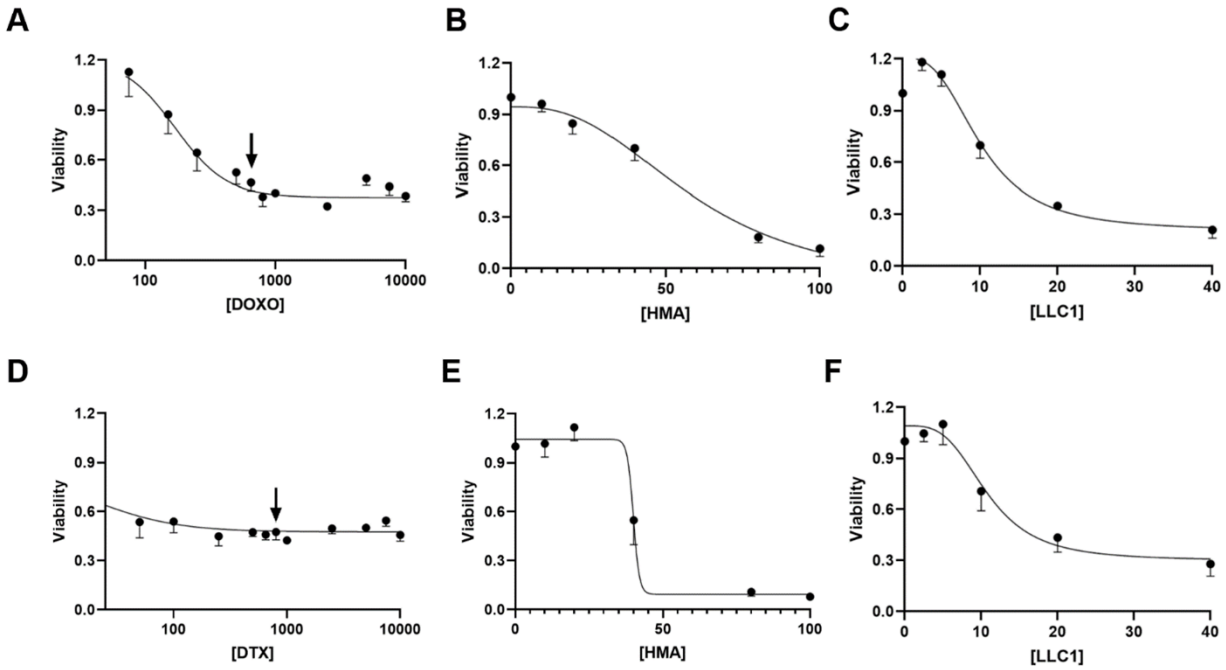

485

486 **Figure 4. LLC1 is cytotoxic toward chemoresistant ER/PR-positive breast cancer cell**

487 **populations.** Dose response curves of T47D cells treated with doxorubicin (DOXO) **(A)** or docetaxel

488 (DTX) **(D)** for 72h are depicted. Populations of cells that persist at drug concentrations higher than

489 650 nM DOXO and 800 nM DTX (arrows) are considered drug resistant. Residual T47D cells that

490 survive treatment with these levels of drugs for 72h were then titrated with HMA **(B, E)** or LLC1 **(C,**

491 **F)** for an additional 24h and viability assessed. Data represent at least three biological replicates.

492

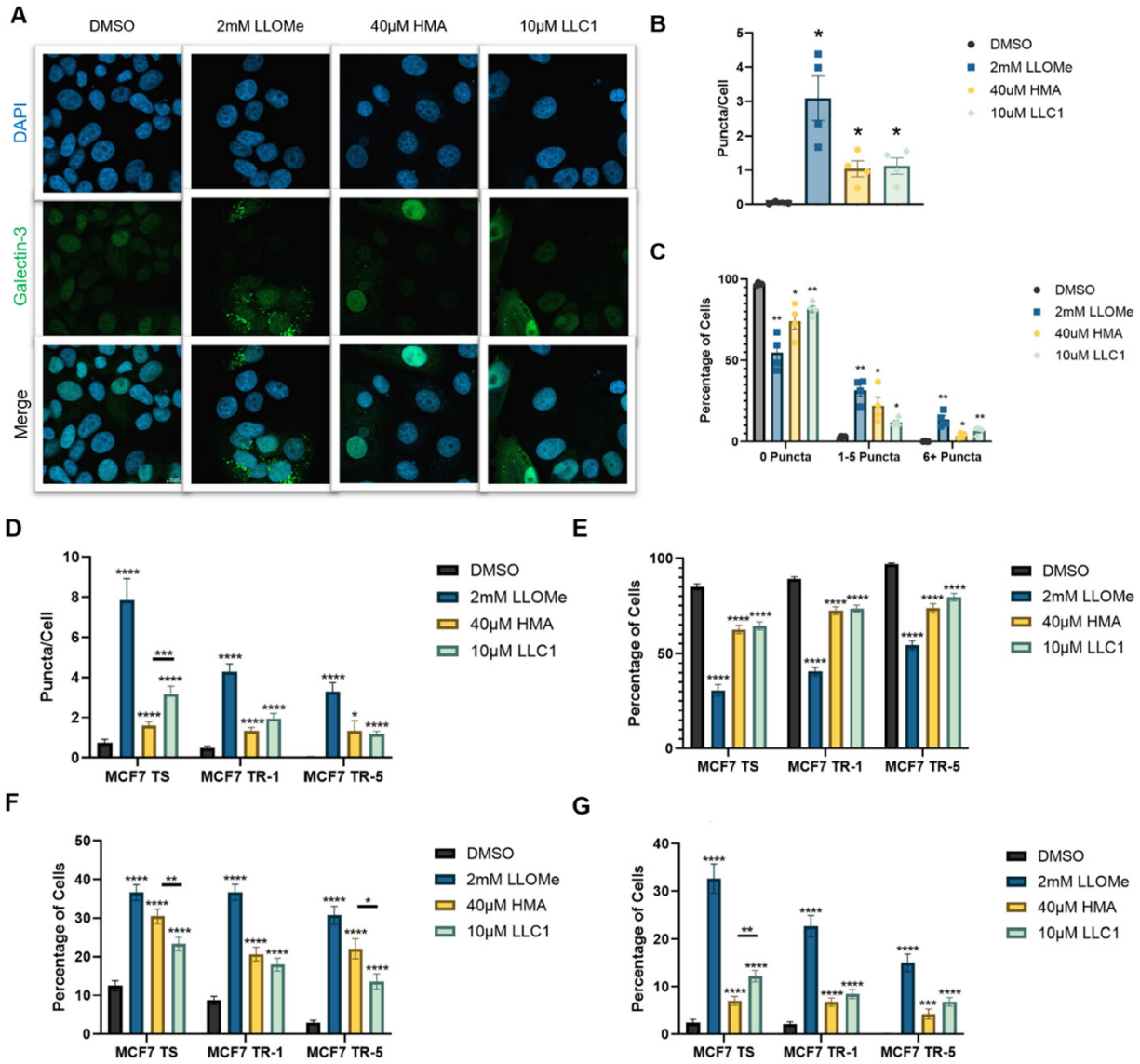

Figure 5. LLC1 induces lysosomal membrane permeabilization in drug-resistant cells. (A-C) MCF7 cells resistant to 5 μM tamoxifen (MCF7 TR-5) cells were treated with vehicle (DMSO), 2 mM LLOMe positive control, 40 μM HMA, or 10 μM LLC1 for 12hr, and galectin translocation into puncta was assessed by confocal fluorescence microscopy. **(A)** Representative images of treated MCF7 TS cells are depicted. Scale bar = 100μm. **(B)** Average puncta per cell was calculated and plotted. **(C)** Percentages of cells exhibiting 0, 1-5 and 6 or more puncta for each drug condition was plotted. **(D-G)** A similar analysis of MCF7 TR-1 and MCF7 TR-5 cells allowed comparisons of average puncta/cell **(D)**, and percentages exhibiting 0 **(E)**, 1-5 **(F)**, or 6 or more **(G)** puncta. Data is

502 compiled from a minimum of four biological replicates from each cell line. *, $P < 0.05$; **, $P < 0.01$;

503 ***, $P < 0.001$; ****, $P < 0.0001$.